Technetium-99m-Tetrofosmin in Dipyridamole-Stress Myocardial SPECT Imaging: Intraindividual Comparison with Technetium-99m-Sestamibi

Patrick Flamen, Axel Bossuyt and Philippe R. Franken

Department of Nuclear Medicine, University Hospital, Free University of Brussels (AZ VUB), Brussels, Belgium

Tetrofosmin is a new ^{99m}Tc-labeled myocardial perfusion imaging agent. Biodistribution studies suggest more favorable heart-to-adjacent organ biokinetics than for ^{99m}Tc-sestamibi after injection during exercise. The aim of this work was to determine intraindividually whether tetrofosmin is more suitable than sestamibi for pharmacological stress testing in a 1-day protocol. **Methods:** Thirty subjects underwent two similar 1-day, rest and dipyridamole stress imaging protocols: one using tetrofosmin, the other using sestamibi. SPECT was performed 60 min after tracer administration. Myocardial images were analyzed both visually and quantitatively. **Results:** Heart-to-liver activity ratios measured on the anterior SPECT projections were significantly higher for tetrofosmin than for sestamibi in the rest and stress studies. Heart-to-lung ratios were similar for both tracers. Significant linear correlations between tetrofosmin and sestamibi perfusion indices were found in normals and in patients with proven or suspected coronary artery disease. In segments showing abnormal uptake during stress, the perfusion indices were similar for tetrofosmin and sestamibi at rest and during stress. The degree of reversibility in these segments was also similar for both tracers. Finally, the extent, intensity and severity of perfusion defects were similar for both tracer studies. **Conclusion:** Tetrofosmin has a more optimal biodistribution than sestamibi when used in a 1-day, rest and dipyridamole stress myocardial SPECT imaging protocol. No significant difference in either the quality or diagnostic interpretation of the images could be demonstrated.

Key Words: technetium-99m-tetrofosmin; dipyridamole; technetium-99m-sestamibi; myocardial perfusion; single-photon emission computed tomography

J Nucl Med 1995; 36:2009–2015

Technetium-99m-tetrofosmin is a lipophilic, cationic diphosphine that has been recently developed for myocardial perfusion imaging. Biokinetic studies have demonstrated rapid clearance from the blood, with excellent cardiac uptake, relatively slow clearance and no significant redistribution (*1–5*). Compared to ^{201}Tl exercise planar imaging, ^{99m}Tc-tetrofosmin offers similar diagnostic accuracy for the detection of coronary artery disease (CAD) (*6,7*). Compared to ^{99m}Tc-sestamibi, tetrofosmin appears to have advantageous characteristics: more convenient labeling procedure at room temperature and more rapid hepatic clearance after exercise injection (*7,8*).

Since tracer uptake kinetics during pharmacological stress testing need not be the same during exercise (*9*), we wondered if tetrofosmin has any advantage over sestamibi in a 1-day, rest and dipyridamole stress imaging protocol. We therefore performed an intraindividual comparison of both ^{99m}Tc-labeled myocardial perfusion agents in a strictly identical 1-day, rest and dipyridamole stress imaging protocol. The study results were evaluated by visual and quantitative image analysis.

MATERIALS AND METHODS

Patients

The study population consisted of 30 patients (18 men, 12 women; mean age 68 ± 10 yr). Five patients had a less than 5% probability for CAD (*10*) and 25 patients had known or suspected CAD. No patient had unstable CAD, significant valvular heart disease, nonischemic cardiomyopathy or left bundle branch block. All patients were in stable clinical condition during the study. The study protocol was approved by the Competent Medical Ethical Committee. Informed consent was obtained from all patients before participation in the study.

Study Protocol

All patients underwent two similar 1-day, rest and dipyridamole stress imaging protocols separated by 48 hr. Tetrofosmin and sestamibi were used as myocardial perfusion agents in a random sequence. Six to 9 mCi were injected intravenously at rest, followed 4 hr later by an injection of 23–28 mCi at maximal dipyridamole stress. The exact amount of injected radioactivity was determined by measuring all injection material before and after radiotracer administration. Myocardial SPECT imaging was started 60 min after the rest and the stress injections. To promote tracer clearance from the gallbladder, patients drank one glass of whole milk or ingested a light, fatty meal before imaging (*11*).

Received Nov. 11, 1994; revision accepted Apr. 12, 1995.

For correspondence or reprints contact: Patrick Flamen, MD, Department of Nuclear Medicine, University Hospital, AZ VUB Laarbeeklaan 101, B-1090 Brussels, Belgium.

Dipyridamole Stress Protocol

Patient preparation was identical to that used in the sestamibi and tetrofosmin studies. All methylxanthine medications and caffeine consumption were discontinued for at least 24 hr before stress testing. Dipyridamole was administered intravenously at a rate of 0.14 mg/kg/min over 6 min for a total of 0.84 mg/kg body weight. Blood pressure, heart rate, EKG and symptoms were monitored before, during and after the pharmacological infusion. Two minutes after the infusion was completed, the radiotracer was injected intravenously. If dipyridamole-related side effects occurred, the infusion was stopped immediately and aminophylline (120 to 240 mg) was injected about 2 min after radiotracer administration (*12*).

Myocardial SPECT Imaging and Processing

Myocardial SPECT imaging was performed using a three-head gamma camera equipped with low-energy, high-resolution parallel-hole collimators that collected 96 separate views over a 360° elliptical arc. The acquisition time per projection was 60 sec for the rest studies and 30 sec for the stress studies. Data were collected in a 128 × 128 matrix on a dedicated computer system. Transaxial slices were reconstructed by filtered backprojection using a Butterworth filter (cutoff frequency 0.35 N, order 5). No attenuation or scatter correction was applied. Transaxial slices were reoriented to obtain oblique angle tomograms parallel to the long and short-axes of the left ventricle.

Visual Analysis

All tomographic images were visually analyzed by two nuclear medicine physicians who were unaware of the patient's clinical records and the radiotracer used. The left ventricular myocardium was divided into nine segments: apex; anterior, septal, inferior and lateral segments on a representative midventricular slice; anterior, septal, inferior and lateral segments on a representative basal slice. For each segment, tetrofosmin and sestamibi uptake were graded semiquantitatively. Scores were attributed on a four-point system by taking into account defect extent and severity. Scores were assigned as follows: 0 (normal uptake) if the activity was 65% or more than that of maximal myocardial activity; 1 (mildly reduced uptake) if activity ranged between 50% and 65% of the maximum; 2 (moderately reduced uptake) if activity ranged between 35% and 50% and 3 (severely reduced uptake) when activity was less than 35% of the maximal activity.

Side-by-side comparative display of the short- and long axis slices was used to categorize the nine segments as: normal (stress score normal), completely reversible (stress score abnormal; rest score normal), partially reversible (stress score abnormal; rest score abnormal but less than stress score) or as fixed defects (stress score abnormal equals rest score, both abnormal). The same scoring system was used for the sestamibi and tetrofosmin studies. Observer disagreement was resolved by consensus after revision.

Myocardial perfusion defects were defined by three parameters: extent (number of myocardial segments within a perfusion defect with a score higher than 0), intensity (highest segmental score within the defect) and severity (sum of all individual scores of abnormal segments within the perfusion defect). These parameters were calculated for the rest and stress images.

Quantitative Image Analysis

Tetrofosmin and sestamibi heart-to-organ ratios were calculated from the anterior projection of each tomographic acquisition. Regions of interest (ROI) were drawn around the entire left ventricular myocardium, over the hepatic margin adjacent to the infero-apical wall of the left ventricle, excluding the biliary tree, and over the left lung parenchyma. The mean counts per pixel in the three ROIs were normalized to the injected tracer activity after decay correction and to a standard acquisition time of 1 min. Heart-to-liver and heart-to-lung ratios were then computed.

Myocardial SPECT images were quantitatively analyzed according to the method proposed by Büll et al. (*13–15*), using the software package installed on the computer system. The left ventricle, from apex to base, was divided into six successive slices, the first of which was fixed at the midapical level in an identical manner for the rest and stress images. The slices were then divided into 33 ROIs by polar mapping, resulting in a target-like display in which the center represented the apex and the outer circle the base of the heart (Fig. 1). Because high variations were usually found in the most basal region, the outer ring with eight ROIs was not considered for further analysis. Stress data were corrected by calculating and subtracting for each slice and ROI the remaining counts from the rest injection, taking into account physical decay, loss of radioactivity from the myocardium (*16*) and the actual ratio of injected radioactivities at rest and during dipyridamole stimulation. Corrected ROI densities were then used to calculate the following parameters: PI rest (%) = perfusion index after resting injection, i.e., the percent uptake in a ROI related to the maximum ROI uptake (100%) in the resting patient dataset; PI stress (%) = perfusion index after stress injection, i.e., the percent uptake in a ROI at stress related to the maximum ROI uptake (100%) in the stress patient dataset.

Rest and stress perfusion indices were then compared to a normal database obtained with sestamibi at rest and during dipyridamole stress in patients with low probability of CAD (Fig. 1). The lower limit of normal was set at the mean minus 2 s.d.s.

Finally, for each patient and radiotracer, the perfusion defects were defined by three parameters: extent (number of abnormal ROIs), intensity (highest difference between the perfusion index of an abnormal ROI and the lower limit of normal of that particular ROI) and severity (sum of all differences between the perfusion indices of the abnormal ROIs and the lower limit of normal of those ROIs). These parameters were calculated for the rest and stress images.

Statistical Analysis

All data are expressed as mean ± s.d.. Univariate analysis of groups was performed by paired Student's t-test or Wilcoxon signed rank test according to the number and distribution of paired observations. Differences between groups of $p < 0.05$ were considered significant. Linear regression analysis was used to compare paired samples. Coefficient of correlations (r) and the s.e.e. are given.

RESULTS

Dipyridamole Stress Results

All 30 study participants completed two dipyridamole stress protocols: one with tetrofosmin, the other with sestamibi. Hemodynamic, clinical and EKG parameters monitored during dipyridamole infusion are listed in Table 1. Blood pressure, heart rate and achieved double product were identical for both stress procedures. The occurrence of anginal chest pain and EKG ischemic changes was also similar.

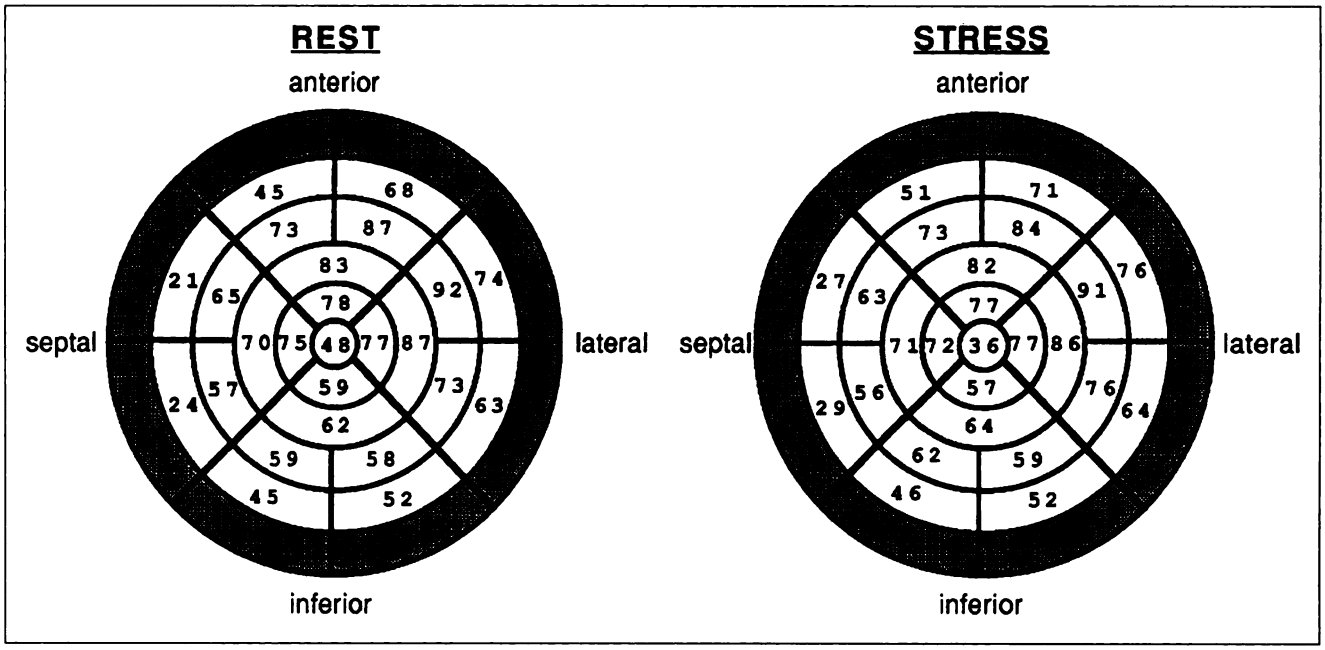

FIGURE 1. Polar maps of the left ventricular myocardium. Numbers reflect the lower thresholds of normal (i.e., mean minus 2 s.d.) of the perfusion indices for sestamibi after rest and dipyridamole stress injection. The center ROI corresponds to the apex. The outer ring (shaded) was not considered for analysis.

Planar Imaging

Good myocardial delineation and adequate contrast between heart and adjacent organs were obtained with both tracers after both rest and dipyridamole stress injection (Fig. 2). Heart, liver and lung activities obtained with tetrofosmin and sestamibi are listed in Table 2. Heart activities were similar with both tracers after rest injection but slightly higher for sestamibi than for tetrofosmin when the tracers were injected during dipyridamole stress (5.77 ± 1.73 versus 4.95 ± 1.56 cts/pixel/min/mCi; $p < 0.001$). In contrast, liver activities were consistently lower with tetrofosmin than with sestamibi, in both the rest and stress studies. Consequently, the heart-to-liver ratios were significantly higher with tetrofosmin than with sestamibi, for both the resting (1.19 ± 0.39 versus 0.96 ± 0.45; $p < 0.05$) and stress studies (1.37 ± 0.37 versus 1.05 ± 0.42; $p < 0.05$). Heart-to-lung ratios were similar for both tracers in the rest (2.91 ± 0.53 versus 2.85 ± 0.65) and stress (3.15 ± 0.65 versus 3.09 ± 0.59) conditions.

TABLE 1
Clinical, Hemodynamic and Electrocardiographic Parameters during Dipyridamole Infusion

Parameter	Sestamibi (±s.d.)	Tetrofosmin (±s.d.)	p value
Systolic blood pressure (mmHg)*	129 (±21)	127 (±18)	ns
Heart rate (bpm)*	92 (±14)	90 (±15)	ns
Double product	11,852 (±2375)	11,478 (±2108)	ns
Stress-induced anginal chest pain	5	6	ns
EKG ischemic changes	7	7	ns
Submaximal dose of dipyridamole†	2	1	ns

*At time of tracer injection.
†Number of patients who received less than the standard dose of dipyridamole (0.84 mg/kg).

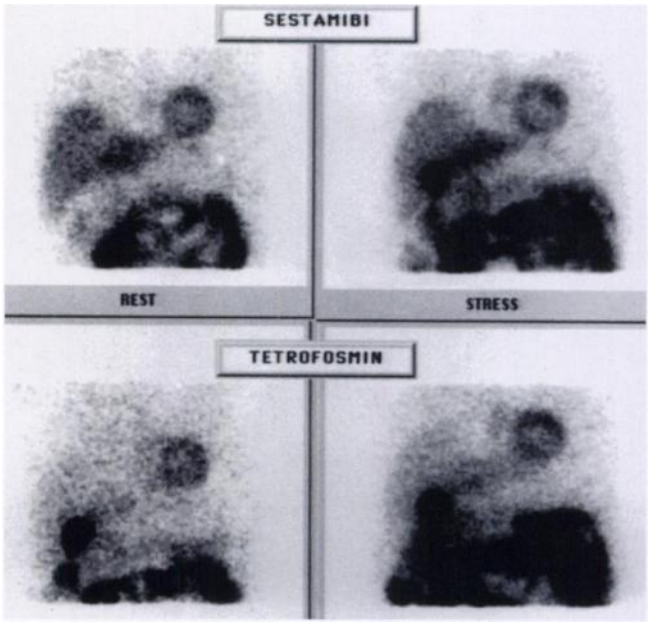

FIGURE 2. Anterior projections of the tomographic acquisitions of rest and stress studies in a patient with suspected CAD. Heart-to-liver activity ratios were better for tetrofosim than for sestamibi, both in the rest (1.5 versus 1.0) and stress study (1.4 versus 1.0).

TABLE 2
Heart, Liver and Lung Activities Measured 60 Minutes after Tracer Administration at Rest and during Dipyridamole Stress

Study	Sestamibi	Tetrofosmin	p value
Rest			
Organ			
Heart	5.12 ± 1.55*	4.97 ± 1.49	ns
Liver	6.13 ± 2.72	4.57 ± 1.92	$p < 0.001$
Lung	1.76 ± 0.45	1.74 ± 0.35	ns
Stress			
Heart	5.77 ± 1.73	4.95 ± 1.56	$p < 0.001$
Liver	6.19 ± 2.72	3.80 ± 1.42	$p < 0.001$
Lung	1.83 ± 0.40	1.59 ± 0.35	$p < 0.001$

*Values are expressed as counts/pixel/minute/mCi (±s.d.).

TABLE 3
Semiquantitative Analysis of Extent, Intensity and Severity of Perfusion Defects on Sestamibi and Tetrofosmin Rest and Stress SPECT Images

Defect	Sestamibi	Tetrofosmin	p value
Extent			
Rest	2.60 ± 1.90	2.65 ± 1.84	ns
Stress	3.55 ± 1.81	3.35 ± 1.73	ns
Intensity			
Rest	1.65 ± 1.18	1.60 ± 0.99	ns
Stress	2.50 ± 1.12	2.55 ± 0.75	ns
Severity			
Rest	4.95 ± 4.77	4.70 ± 4.49	ns
Stress	7.35 ± 5.55	7.10 ± 5.14	ns

Visual Analysis

High-quality SPECT images with good myocardial delineation were obtained with both tracers after the rest and dipyridamole stress injections. A typical example of a dipyridamole-induced perfusion defect in the infero-lateral wall is shown in Figure 3. In two patients, however, SPECT images were considered unsuitable for evaluation due to an overlapping intestinal activity on the infero-apical myocardial wall in the sestamibi (one patient) and tetrofosmin (one patient) studies. These two patients were therefore excluded from further analysis.

The results of the semiquantitative analysis of the images are listed in Table 3. The extent, intensity and severity of the myocardial perfusion defects on the rest and dipyridamole stress images were similar for both radiotracers.

Comparison of the diagnostic interpretation of the sestamibi and tetrofosmin images was performed on a patient and segmental basis (Fig. 4). Of the 28 patients, 8 were classified as normal in both tracer studies. Overall concordance of diagnostic classification was present in 79% of the 28 patients. In patients showing either abnormal sestamibi or tetrofosmin uptake during dipyridamole stress, diagnostic categorization was concordant in 70% of the patients. When the results were discordant, there was no significant systematic trend.

Segmental analysis identically classified 94.4% of the 252 segments as normal, partially reversible, totally reversible or fixed defect in both tracer studies. Of the 68 segments showing abnormal uptake of either tetrofosmin or sestamibi during dipyridamole stress, diagnostic categorization was concordant in 54 segments (79.4%): 12 segments showed total reversibility, 8 segments partial reversibility and 34 segments fixed defects. When results were discordant, there was no systematic trend: 7 of the 41 segments with fixed defects (sestamibi study) showed reversibility with tetrofosmin, whereas 5 of the 39 segments with fixed defects (tetrofosmin study) showed reversibility with sestamibi.

Quantitative Analysis

In the five patients with low probability of CAD, excellent linear correlation between the segmental perfusion indices of both tracer studies was found at rest ($r = 0.95$) and during stress ($r = 0.94$). In these patients, paired

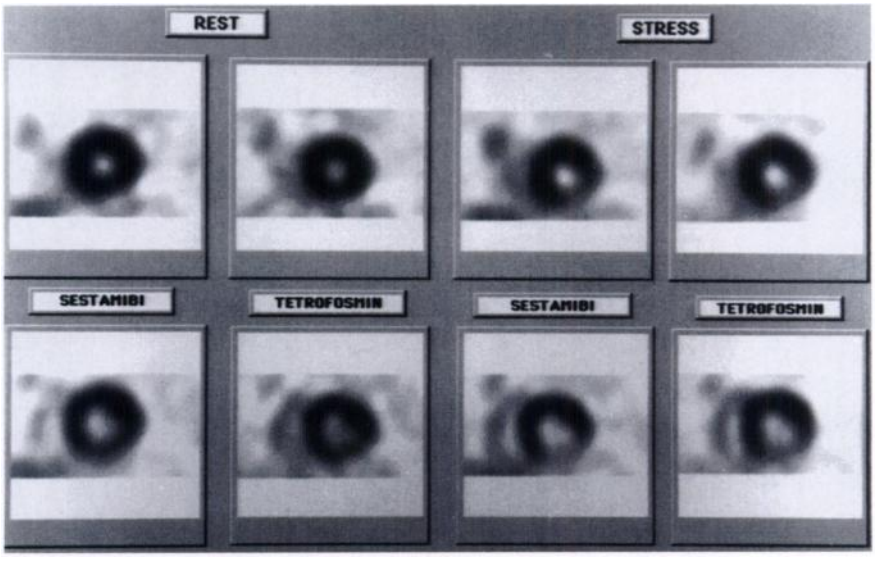

FIGURE 3. Comparative display of short-axis SPECT images obtained 60 min after administration of sestamibi and tetrofosmin at rest and during dipyridamole stress in a patient with suspected CAD. The upper images represent midventricular and the lower images basal myocardial slices. Similarities of defect extent, intensity and severity were demonstrated.

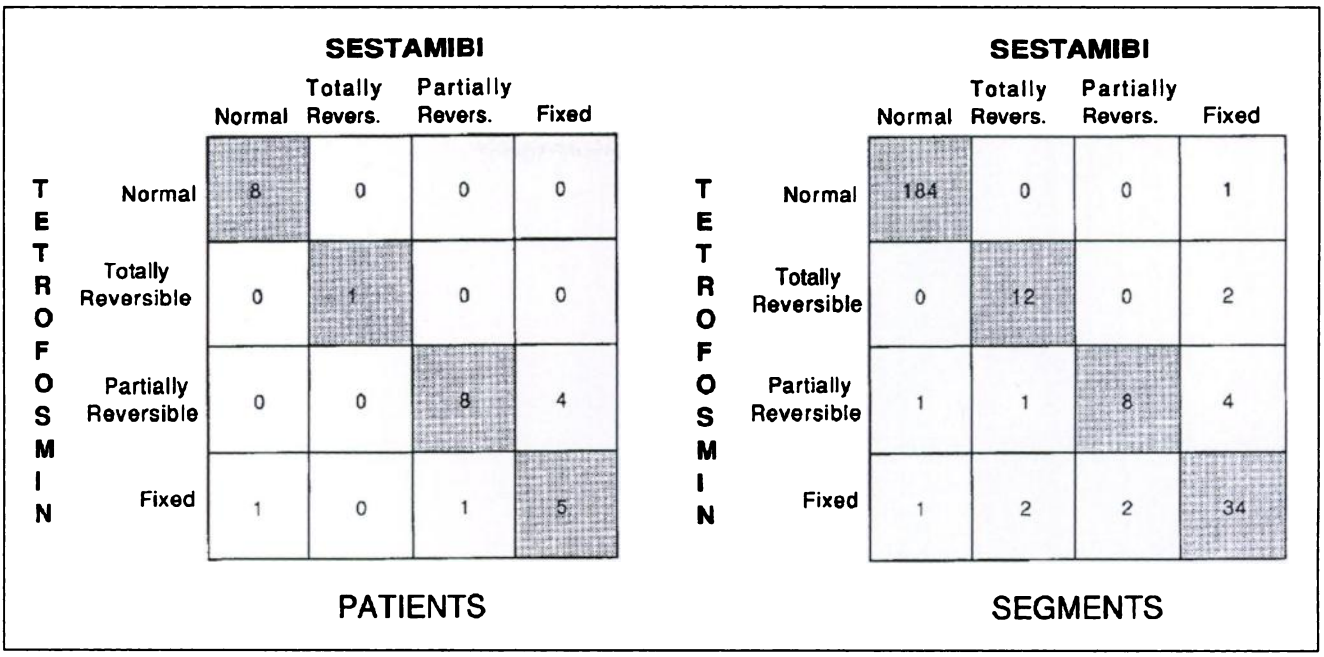

FIGURE 4. Concordance data of diagnostic classification of patients and segments between sestamibi and tetrofosmin studies.

comparison of all perfusion indices (n = 125) did not demonstrate any difference between tetrofosmin and sestamibi at rest (76.29 ± 14.87 and 77.10 ± 14.48, respectively; p = ns) or during dipyridamole stimulation (76.50 ± 15.45 and 77.35 ± 14.65, respectively; p = ns) (Fig. 5). The perfusion indices of the sestamibi rest and dipyridamole stress images in these patients were all within normal limits.

Similar highly significant linear correlations between tetrofosmin and sestamibi perfusion indices were also observed in the patients with proven or suspected CAD (r = 0.92).

In segments showing abnormal tetrofosmin or sestamibi uptake during stress (n = 157), the perfusion indices were similar for both tracers at rest (66.76 ± 17.18 and 66.68 ± 16.38, respectively; p = ns) and stress (60.47 ± 15.66 and 59.70 ± 16.63, respectively; p = ns) (Fig. 6). The degree of reversibility of these abnormal segments, calculated as the difference between perfusion indices at rest and stress, was similar for both tracers (6.29 ± 7.67 for tetrofosmin and 6.97 ± 9.26 for sestamibi; p = ns).

The extent, intensity and severity of the perfusion defects calculated at rest and during dipyridamole stimulation for sestamibi and tetrofosmin are listed in Table 4. No significant differences were found in any of these parameters.

A ratio of the mean perfusion index of the eight inferior and infero-septal segments to the eight anterior and antero-

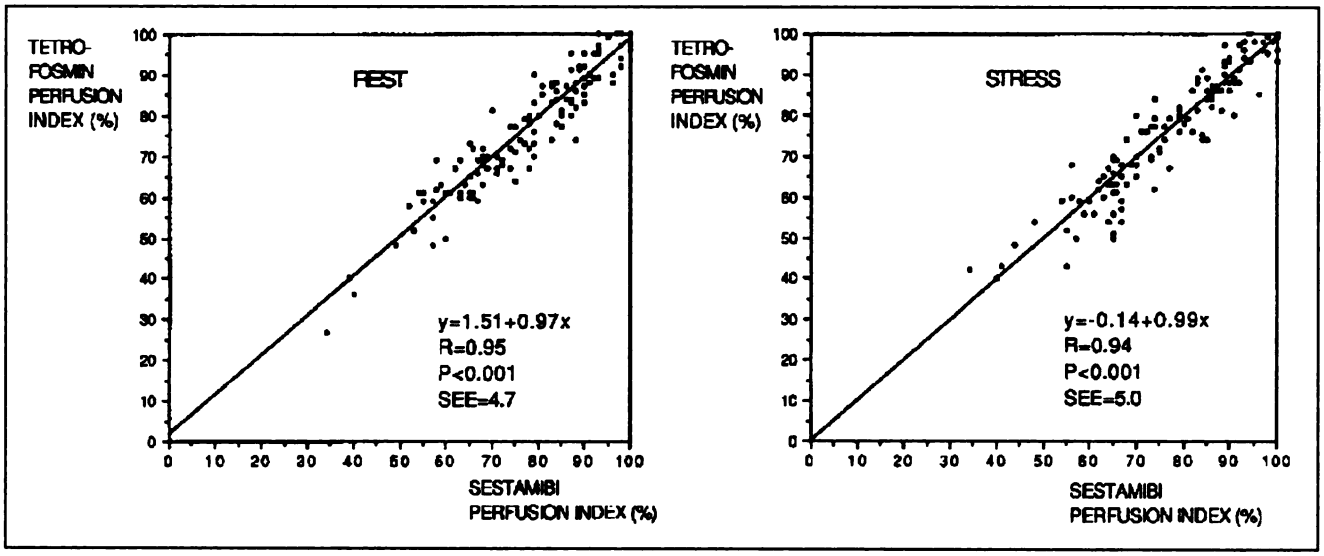

FIGURE 5. Quantitative SPECT image analysis. Linear correlation between segmental perfusion indices of sestamibi and tetrofosmin at rest (left) and stress (right) in patients with low probability of CAD.

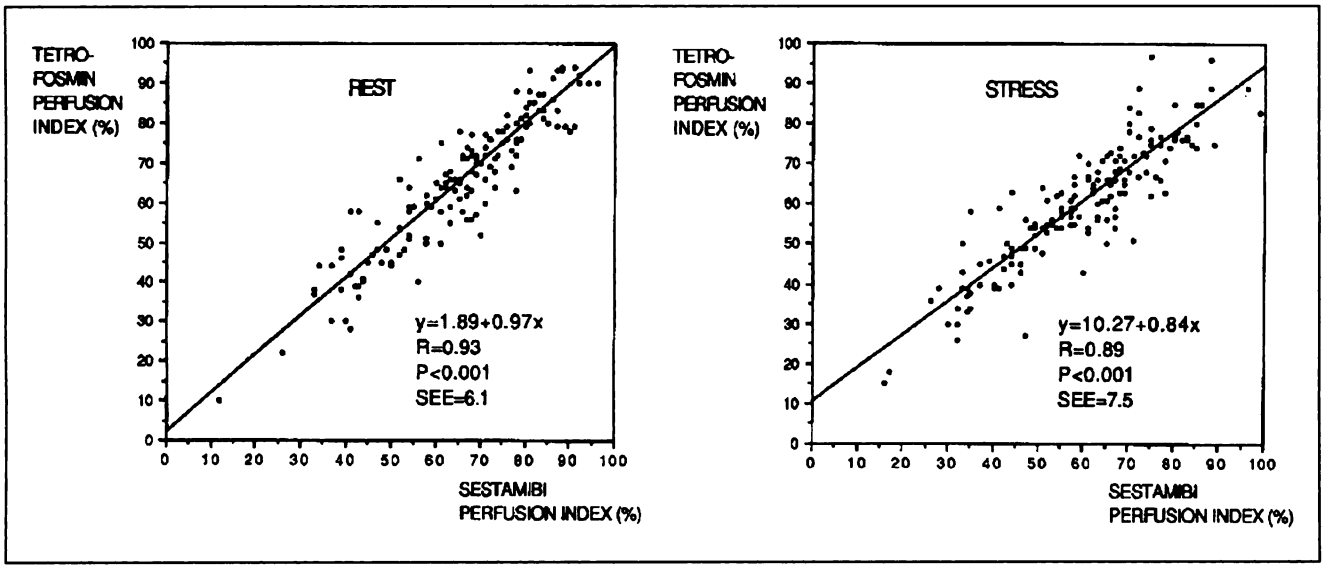

FIGURE 6. Quantitative SPECT image analysis. Comparison of perfusion indices of myocardial segments with either sestamibi or tetrofosmin abnormal uptake at rest (left) and stress (right).

lateral segments was calculated in both tracer studies. Similar ratios were found for both tracer studies at rest (0.79 ± 0.20 and 0.79 ± 0.19, respectively; p = ns) and during stress (0.80 ± 0.23 and 0.79 ± 0.22, respectively; p = ns).

DISCUSSION

Intraindividual comparison of biodistribution data of tetrofosmin and sestamibi obtained 1 hr after rest and dipyridamole stress injections indicated more optimal heart-to-liver ratios for tetrofosmin in both conditions. This is primarily due to an important difference in liver radioactivity, which is consistently lower when tetrofosmin is used. Myocardial uptake values of tetrofosmin after dipyridamole stress injection were lower compared to sestamibi.

Early reports on the biokinetics of tetrofosmin after injection during exercise indicated extremely rapid tracer clearance from the hepatic parenchyma. At 30 and 60 min after tracer injection during exercise, Jain et al. (*2*) reported heart-to-liver ratios of 1.4 ± 0.3 and 1.6 ± 0.4, respectively; whereas Higley et al. (*1*) reported ratios of 1.2 ± 0.7 and 3.1 ± 3, respectively. These ratios compare more favorably to the heart-to-liver ratios obtained in our study, in which tetrofosmin was injected during dipyridamole infusion (1.37 ± 0.4 at 60 min after injection). Moreover, preliminary results of biokinetic studies of tetrofosmin after dipyridamole stress injection reported by our group (*17*) indicate suboptimal heart-to-liver ratios when imaging is performed at 30 min (0.78 ± 0.09 at 30 min postinjection). In aggregate, these data suggest that the biokinetics of tetrofosmin depend on the applied stress condition. Similar findings have also been reported for sestamibi. Taillefer (*9*) studied the biodistribution of sestamibi, both after exercise and dipyridamole stress injections in the same patient population. Sixty minutes after tracer injection during treadmill exercise, the heart-to-liver ratio was 1.9 ± 0.5, whereas the ratio was 1.3 ± 0.3 ($p < 0.001$) when the tracer was injected during dipyridamole stress. This difference in tracer kinetics is probably due to increased muscular tracer sequestration during exercise, resulting in lower hepatic tracer uptake.

TABLE 4
Quantitative Analysis of Extent, Intensity and Severity of Perfusion Defects on Sestamibi and Tetrofosmin rest and stress SPECT Images

Defect	Sestamibi	Tetrofosmin	p value
Extent			
Rest	2.82 ± 3.62	2.89 ± 3.68	ns
Stress	4.11 ± 3.84	4.14 ± 4.13	ns
Intensity			
Rest	7.64 ± 10.85	8.11 ± 10.33	ns
Stress	12.39 ± 13.49	10.86 ± 12.48	ns
Severity			
Rest	26.07 ± 51.78	29.50 ± 47.21	ns
Stress	50.43 ± 73.66	43.46 ± 63.70	ns

The importance of the heart-to-liver activity ratio for good quality myocardial perfusion SPECT images lies in the fact that filtered backprojection causes artifactually decreased activity of the inferior-inferoseptal myocardial wall in the reconstructed images (*18–19*). The artifact observed in the heart is proportional to the heart-to-liver activity ratio. On the other hand, part of this artifactual count decrease effect is probably mitigated by Compton scatter of hepatic and intestinal photons resulting in the SPECT system's overestimation of tracer uptake in a myocardial perfusion defect (*20*). To assess whether the difference in heart-to-liver ratios between sestamibi and tetrofosmin is important enough to influence measured myocardial counts, we compared the perfusion indices of the eight inferior and infero-septal segments (the most

susceptible to the artifact as they are closest to the liver) of rest and stress images. In our study, however, no difference between the two tracers could be detected, suggesting that the advantage of tetrofosmin biodistribution is too modest to influence image quality, at least after injection during dipyridamole stress.

Comparative quantitative SPECT image analysis, using the method described by Büll (*13–16*), demonstrated excellent and identical linear correlations between the segmental perfusion indices of both normal and hypoperfused segments, as observed in the rest and stress studies. The correlation was slightly weaker in the hypoperfused segments in the stress studies. This variation of regional tracer uptake was probably due to slight differences in stress between both tracer studies and not to differences in tracer characteristics. Moreover, we could not demonstrate any significant difference in the extent, intensity, severity or degree of reversibility of the myocardial perfusion defects between tetrofosmin and sestamibi studies. These data, however, should be regarded cautiously. Because no reference database for tetrofosmin studies was at our disposal, the data obtained with this tracer were compared to a database of normal values set up for sestamibi. Nevertheless, the potential bias of doing so seems to be limited since a similar distribution pattern of both radiotracers through the myocardium was demonstrated in the normal control patients included in the study.

CONCLUSION

This clinical study assessed the diagnostic value of tetrofosmin by intraindividual comparison with sestamibi in strictly comparable clinical and technical circumstances. High concordance in the detection of ischemic and scarred myocardium was obtained, suggesting a similar diagnostic value for both radiotracers. We did not attempt to study the absolute diagnostic accuracy of tetrofosmin, because definitive conclusions in this regard can only be drawn by studying larger patient cohorts. Nonetheless, our results indicate that tetrofosmin offers better biodistribution than sestamibi when used in a 1-day rest and dipyridamole stress myocardial SPECT imaging protocol. Moreover, no significant difference in either the quality or diagnostic interpretation of the images could be demonstrated.

ACKNOWLEDGMENTS

The authors thank the staff of the Department of Nuclear Medicine, University Hospital of Brussels (AZ VUB), for their enthusiastic cooperation. They also thank Amersham International, plc, for providing the tetrofosmin (Myoview™) and Dr. Bernheim Jan for proofreading the manuscript.

REFERENCES

1. Higley B, Smith FW, Smith T, et al. Technetium-99m-1,2-bis(bis((2-ethoxyethyl)phosphino)ethane: human biodistribution, dosimetry and safety of a new myocardial perfusion imaging agent. *J Nucl Med* 1993;34:30–38.
2. Jain D, Wackers FJTh, Mattera J, et al. Biokinetics of technetium-99m-tetrofosmin: myocardial perfusion imaging agent: implications for a one-day imaging protocol. *J Nucl Med* 1993;34:1254–1259.
3. Kelley JD, Forster AM, Highley B, et al. Technetium-99m-tetrofosmin: a new radiopharmaceutical for myocardial perfusion imaging. *J Nucl Med* 1993;34:222–227.
4. Sridhara BS, Braatt S, Itti R, Rigo P, Cload P, Lahiri A. Early and late myocardial imaging with a new technetium-99m diphosphine (PPN 1011) in coronary artery disease [Abstract]. *J Am Coll Cardiol* 1992;19:202A.
5. Jain D, Wackers FJTh, McMahon M, Zaret BL. Is there any redistribution with Tc-99m-tetrofosmin imaging? A quantitative study using serial planar imaging [Abstract]. *Circulation* 1992;86:I–46.
6. Tamaki N, Takahashi N, Kawamoto M, et al. Myocardial tomography using technetium-99m-tetrofosmin to evaluate coronary artery disease. *J Nucl Med* 1994;35:594–600.
7. Rigo P, Leclercq B, Itti R, Lahiri A, et al. Technetium-99m-tetrofosmin myocardial imaging: a comparison with thallium-201 and angiography. *J Nucl Med* 1994;35:587–593.
8. Wackers FJTh, Berman DS, Maddahi J, et al. Technetium-99m hexakis 2-methoxyisobutyl isonitrile: human biodistribution, dosimetry, safety and preliminary comparison of thallium-201 for myocardial perfusion imaging. *J Nucl Med* 1989;30:301–311.
9. Taillefer R. Technetium-99m-sestamibi myocardial imaging: same-day rest-stress studies and dipyridamole. *Am J Cardiol* 1990;66:80E–84E.
10. Diamond A, Forrester JS. Analysis of probability as an aid in the clinical diagnosis of coronary artery disease. *N Engl J Med* 1979;300:1350–1358.
11. Garcia E, Cooke D, Van Train K, Folks R, et al. Technical aspects of myocardial SPECT imaging with technetium-99m-sestamibi. *Am J Cardiol* 1990;66:23E–31E.
12. Botvinick E, Dae M. Dipyridamole perfusion scintigraphy. *Semin Nucl Med* 1991;3:242–265.
13. Stirner H, Büll U, Kleinhans E. Three-dimensional ROI-based quantification of stress/rest ^{201}Tl myocardial SPECT: presentation of a method. *Nuklearmedizin* 1986;25:128–133.
14. Büll U, Stirner H, von Dahl J, et al. Quantitative evaluation of myocardial stress/rest Tl-201 SPECT: results of a ROI-based method in 108 patients with CHD. *Nuklearmedizin* 1987;26:234–240.
15. Büll U, Dupont F, Uebis R, et al. Technetium-99m-methoxy-isobutyl-isonitrile SPECT to evaluate a perfusion index from regional myocardial uptake after exercise and at rest. Results of a four-hour protocol in patients with coronary heart disease and in controls. *Nucl Med Commun* 1990;11:77–94.
16. Stirner H, Büll U, Kleinhans E, et al. Myocardial kinetics of Tc-99m-hexakis-(2-methoxy-isobutyl-isonitrile) (HMIBI) in patients with coronary heart disease: a comparative study versus ^{201}Tl with SPECT. *Nucl Med Commun* 1989;9:15–23.
17. Flamen P, De Sadeleer C, Rosseel M, Bossuyt A, Franken PR. Comparison between Tc-99m-tetrofosmin and Tc-99m-sestamibi for dipyridamole stress test using a one-day imaging protocol [Abstract]. *Eur J Nucl Med* 1994;8:758A.
18. Germano G, Chua T, Kiat H, et al. A quantitative phantom analysis of artifacts due to hepatic activity in technetium-99m myocardial perfusion SPECT studies. *J Nucl Med* 1994;35:356–359.
19. Nuyts J, Dupont P, Van den Maegdenbergh V, et al. A study of the liver-heart artifact in emission tomography. *J Nucl Med* 1995;36:133–139.
20. Chang W, Henkin R, Buddenmeyer E. The sources of overestimation in the quantification by SPECT of uptakes in a myocardial phantom: concise communication. *J Nucl Med* 1984;25:788–791.